Particle Reduced, Efficient Gasoline Engines

EUROPEAN COMMISSION
Horizon 2020 | GV-2-2016 | Technologies for low emission light duty powertrains
GA # 723954

Deliverable No.	PaREGEn D1.12	
Deliverable Title	Fast 0D simulation method and models for the virtual sensors adapted to the demonstrator engines	
Deliverable Date	2019-07-31	
Deliverable Type	REPORT	
Dissemination level	Public (PU)	
Written By	Christophe Barro (ETH)	2019-07-29
Checked by	Andreas Manz (BOSCH)	2019-07-30
Approved by	Andreas Manz (BOSCH) Vincent Thomas (SIEMES) Simon Edwards (RIC) - Coordinator	2019-07-30 2019-07-30 2019-07-31
Status	Final	2019-07-31

Publishable Summary

Particle formation is a complex process, especially in spark ignition engines. The chemical process of soot formation contains multiple important steps. In direct injection spark ignition engines, the known sources of particulate matter (PM) formation are pool fire locations, coming from piston or wall interaction with liquid fuel, as well as from insufficient air-fuel-mixing. It is also known that at very low load conditions or even during motoring, the majority of particles are not soot but come from wear and lube oil. The interaction between soot and non-soot particles is not yet fully understood.

In the present work, a virtual Gasoline Particle Sensor (vGPS) has been developed in Work Package 1 (WP1, Advanced Combustion Technologies) of the PaREGEn project. Within this work package, novel detailed 3D and 1D/0D modelling approaches, as well as laser diagnostics for liquid fuel film and soot quantification in optical engines, are used to further understand the soot formation process in direct injected spark ignition engines. The detailed models are combination of a validated flow field model, containing the local distribution of the mixture fraction as well as temperature including phenomena like spray-wall interaction or cycle to cycle variations, and a soot chemistry model. The goal of this particular sub-task of WP1 is to use the detailed models and measurements to gain understanding and generate relationships to develop a fast model. The fast model shall be able to run in real time on an electronic control unit (ECU) as a virtual Gasoline Particle Sensor, to enable online strategy adaptations or emission feedback control.

The vGPS contains sub-models to describe the dominant phenomena for the soot formation and oxidation processes. The sub-models are used to estimate the fuel mass, which is present under fuel rich conditions, the cylinder pressure and temperature, and a time scale as inputs for a soot model, calculating soot formation and soot oxidation. The phenomena included in sub-models are air-fuel mixing, wall impingement and evaporation, combustion and heat transfer. Unknowns and engine specific phenomena are addressed with model parameters, which need to be calibrated.

The vGPS has been calibrated on a single cylinder engine as well as a multi cylinder engine under steady state conditions. The engine operation includes stoichiometric, lean and fuel rich conditions. The calculated soot emissions are in good agreement with the measurements. The calculation duration of one engine cycle requires approximately 5 ms on a state of the art laptop. The vGPS has been successfully integrated into the simulation software Siemens Simcenter Amesim.

Contents

Figures

1 Introduction

1.1 Motivation for a virtual gasoline particle sensor

Particle formation is a complex process, especially in spark ignition engines. The chemical process of soot formation contains multiple important steps. In direct injection spark ignition engines, the known sources of PM formation are pool fire locations, coming from piston or wall interaction with liquid fuel, as well as from insufficient air-fuel-mixing. It is also known that at very low load conditions or even during motoring, the majority of particles are not soot but come from wear and lube oil. The interaction between soot and non-soot particles is not yet fully understood. A virtual Gasoline Particle Sensor (vGPS) enables real time estimations of particle number (PN), calibrated with testbench results. These estimations can be used to avoid high PN emissions during transient operation or cold starts.

1.2 Objective and Goal

Based on the elaborated soot formation mechanisms derived in Task 1.4 of WP1, the goal of the task reported here was to develop a highly abstracted soot model capable of calculation in time for real-time estimations on a state of the art ECU or a suitable simulation environment. The outcome is a model using this highly abstracted process description plus model parameters, which need to be calibrated using PM and/or PN measurements in the exhaust gas. Once the model is calibrated on the demonstrator engines, it is able to run on-line as a virtual sensor.

2 Methods and results

2.1 vGPS Concept

The concept of the vGPS foresees the application of a phenomenological soot model, typically applied in a diesel engine. These types of soot models typically contain a term for soot formation as well as for soot oxidation (equation 1). The term for soot formation mainly depends on the fuel mass that is present under (locally) fuel rich conditions. In a diesel engine, this can be determined from the fuel mass, which is converted in a mixing controlled type of combustion.

$$\frac{dm_{Soot}}{dt} = \frac{dm_{Formation}}{dt} - \frac{dm_{Oxidation}}{dt} \quad (1)$$

$$\frac{dm_{Formation}}{dt} = A_f \cdot m_{fg} \cdot p^{0.5} \cdot e^{-\left(\frac{E_{sf}}{R \cdot T}\right)} \quad (2)$$

$$\frac{dm_{Oxidation}}{dt} = A_o \cdot m_s \cdot \frac{p_{O_2}}{p} \cdot p^{1.8} \cdot e^{-\left(\frac{E_{so}}{R \cdot T}\right)} \quad (3)$$

In both the formation and oxidation terms (example from Hiroyasu [1], equations 2 and 3, respectively), the model considers a scaling constant A, a concentration dependency (m_{fg} representing the evaporated fuel in the formation) an m_s, the already formed soot, as well as the oxygen partial pressure in the oxidation term, a cylinder pressure dependency (p) with empirical exponents and an Arrhenius term.

In contrary, in a direct injected gasoline engine, it is less trivial to find fuel rich combustion portions. Therefore, a set of sub-models are required to estimate the correct boundary conditions for the soot model. Figure 2-1 shows an overview of the model concept. The fuel mass, which is present under fuel rich conditions ($m_{critical}$), is estimated using a spray model, an impingement model and an evaporation model. The temperature, the pressure and the oxygen concentration are gathered from a combustion and a heat transfer model. The model inputs are all variables, which are available on a standard electronic control unit (ECU). The model parameters need to be calibrated using steady state particulate number (PN) measurements (or derived values) from a test bench.

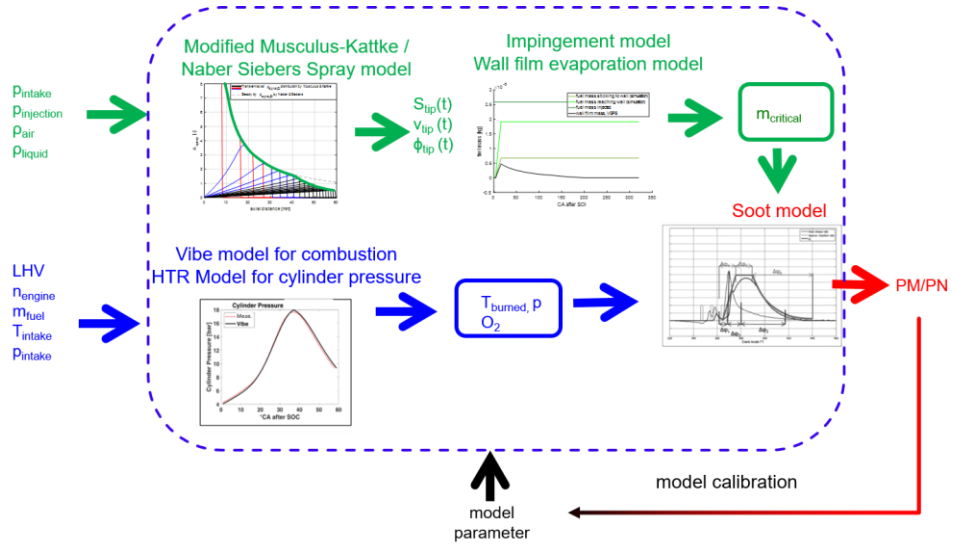

Figure 2-1 Model Concept Overview

2.1.1 Soot model

The soot model used has been developed for a passenger car diesel engine for real time estimations. Additional details to the description below can be found in [2, 3]. The soot formation and oxidation process are, for simplicity reasons, regarded as consecutive processes. The model itself deals with three different steps:

- Formation dominating phase
- Equilibrium phase
- Oxidation dominating phase.

The formation dominating phase is only dependent on the fuel mass that is present under fuel rich conditions (local conditions in a diffusion combustion in diesel engines). The phase in the soot evolution, where soot formation and soot oxidation occur, is represented in the equilibrium phase. In the model, soot formation and oxidation appear in balance and do not change the soot concentration. The soot oxidation is approximated in the oxidation dominating phase with an exponential decrease of soot concentration. The shape of the exponential function is manly affected by the temperature, the oxygen availability, the turbulence and the fuel mass. The time scale of each of these phases is obtained using characteristic points out of the heat release rate. The characteristic oxidation temperature is calculated using the cylinder pressure by applying the ideal gas law after a charge mass estimation.

Using the described phases and, in total,12 parameters (b1 – b12) that need to be calibrated with exhaust gas soot measurements, the model equations turn to:
Formation:

$$m_{Soot,Form} = b_1 \cdot m_{fuel,diff}^{\,b_2} \tag{4}$$

The soot formation becomes proportional to the fuel mass participating at the diffusion flame, respectively the fuel mass present under fuel rich conditions.
Equilibrium phase:

$$m_{Soot,Equilibrium} = m_{Soot,Form} \cdot \left(1 + 0 \cdot \left(\frac{\Delta\varphi_2}{\varphi_{ref}} \right)^{6\,7^{\Delta\varphi_5}8} \right) \tag{5}$$

The modelled soot mass does not change during the equilibrium phase. Its duration is described by Δϕ5. ϕref is set to 1° crank angle. This calculation is only necessary if the in-cylinder soot trace is required. For exhaust calculation only, it can be skipped.
Oxidation:

$$m_{Soot,End} = m_{Soot,Eq} \cdot \left(0.01 + \exp\left(-B \cdot \left(\frac{b_{12} \cdot \Delta\varphi_3}{\varphi_{ref}} \right)^{64\,7^{\Delta\varphi_6}8} \right) \right) \tag{6}$$

$$B = \left(\frac{T_{ox}}{T_{ref}} \right)^{b3} \cdot \left(1 + b_4 \cdot EGR_{stoic} \right)^{-b5} \cdot \left(\frac{b_6 \cdot \lambda}{2} \right)^{b7} \cdot \left(\frac{p_{rail}}{p_{rail,ref}} \right)^{b8} \cdot \left(\frac{5}{\sin\left(IPS \cdot \frac{\pi}{2} \right)} \right)^{b9} \cdot \left(\frac{rpm}{rpm_{ref}} \right)^{b10} \cdot \left(\frac{m_{fuel}}{m_{fuel,ref}} \right)^{b11} \tag{7}$$

The soot oxidation is estimated with an exponential decay of the formed soot within the time Δϕ6. This time is depending on the combustion duration. The factor, how fast the soot is oxidized (B) in equation 6 or 7, contains a reaction kinetics component and a turbulence component. This model has only been slightly adapted for the use in gasoline direct injection (GDI) engines. The parameters b4, b5, b9 and b11 have been set to 0 and the stoichiometric air to fuel ratio λ has been modified to λ-1. This inhibits soot oxidation if oxygen is not available. As previously mentioned, for the application in a GDI engine, the estimation of the fuel mass ($m_{fuel,diff}$ in equation 4, for GDI application stated as $m_{critical}$) is different. The critical fuel mass is defined as the fuel mass that is present under conditions which are known to form soot. This is defined here as fuel that is present with an equivalence ratio between 2 and 6. Therefore, the state of mixing is required.

2.1.2 Spray model

The usage of a spray model allows an estimation of the state of mixing of the fuel at the start of the combustion. Here two different spray models have been considered. Firstly, the spray model of Naber & Siebers [4], which provides the spray axis equivalence ratio distribution in a computationally very efficient manner, but for a continuous spray. The second is the 1D spray model from Musculus & Kattke [5]. This model shows the ability to capture the transient spray behaviour after the end of injection.

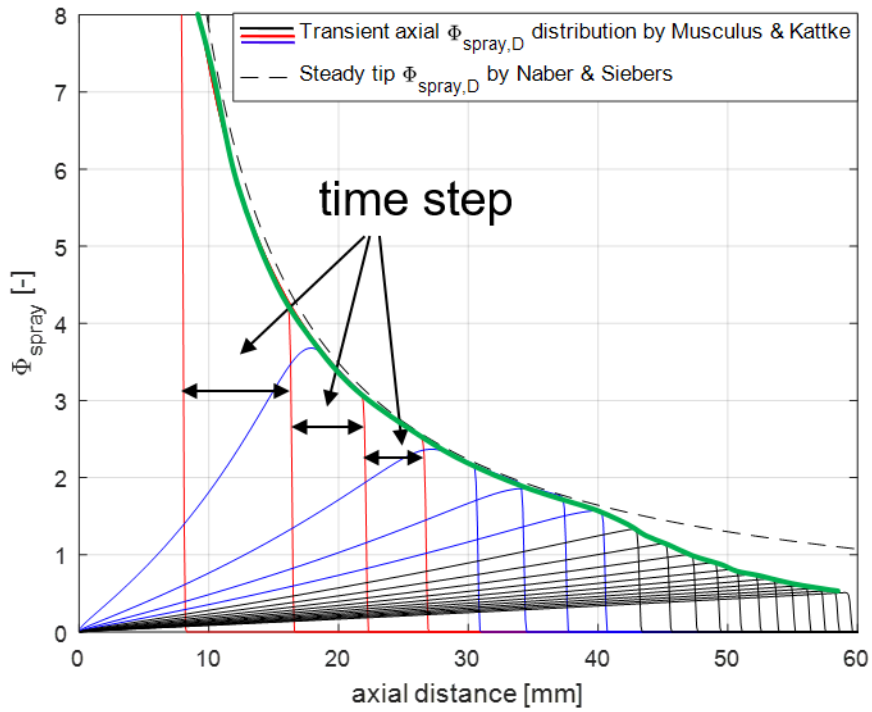

Figure 2-2 Spray model overview using exemplary operating condition

Approximation of the two spray models

In order to reduce computational time for the virtual soot sensor, a power function $f(x) = a \cdot x^b + c$ describes the ratio between the steady state Naber & Siebers equivalence ratio curve and the transient Musculus Kattke equivalence ratio curve. Therefore, the curve by Nabers & Siebers is multiplied by the power function starting from where the entrainment wave hits the jet. This transition point is estimated as a function of the injection time $CA_{transition} = f_{delay} \cdot DOI$, where DOI is the injection duration in crank angles and f_{delay} is a constant equal to 2.3. Since these spray models describe the equivalence ratio distribution into a pressurized

environment with infinite size, the equivalence ratio curve converges towards zero. Therefore, the assumption of fuel re-entrainment is set. As soon as the spray hits the wall or the piston, the spray starts to re-entrain into itself. A linear increase of the equivalence ratio is introduced, starting from the point of impingement and the approximate global equivalence ratio. Figure 2-3 demonstrates the combination of the spray models: the black dotted line shows the Naber & Siebers model, the green curve shows the spray tip equivalence ratio of all time steps of the Musculus & Kattke model. The red line shows the Naber & Siebers model, multiplied with the power function, the blue line shows the final result, when re-entrainment is included as well. The blue curve represents the tip equivalence ratio and spray penetration length for all further calculation.

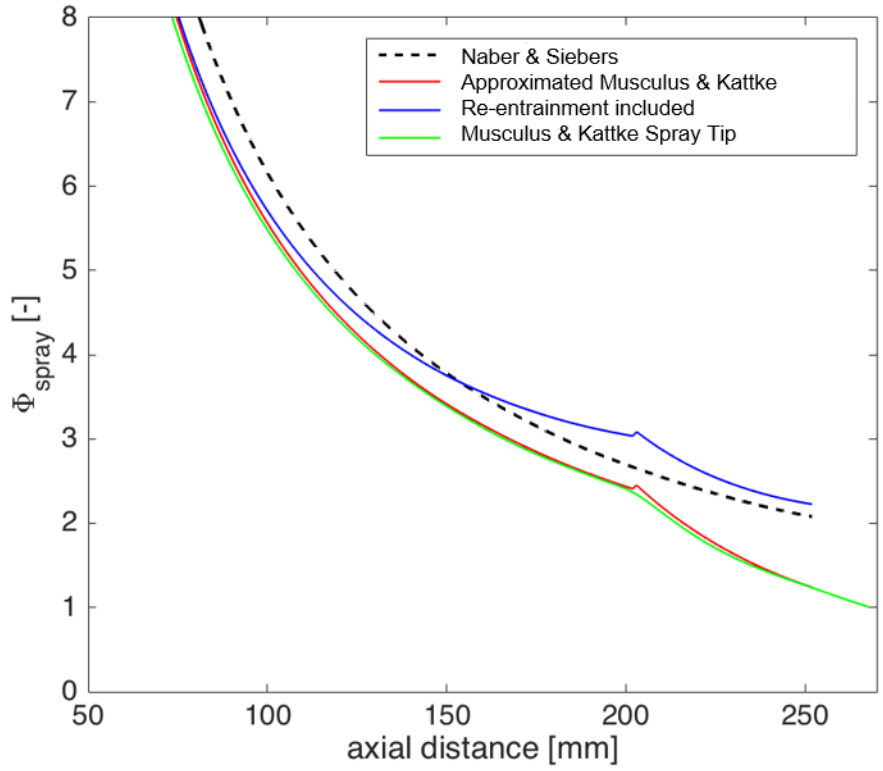

Figure 2-3 Naber & Siebers (black dotted), Musculus & Kattke (green), "fast" Musculus & Kattke approximation (red) and "fast" Musculus & Kattke approximation including re-entrainment of fuel into the spray

2.1.3 Impingement Model

The impingement model by Bai & Gosman [6] for wetted walls differentiates four regimes determined by the Weber number:

- Stick: We ≤ 2
- Rebound: 2 < We ≤ 20
- Spread: 20 < We ≤ We_c
- Splash: We_c < We

$$We = \frac{\rho_l * d_d * {v_{in}}^2}{\sigma} \tag{8}$$

$$We_c = 1320 * La^{-0.18} \tag{9}$$

$$La = \frac{\rho_l * \sigma * d_d}{\mu^2} \tag{10}$$

where,
We is the Weber number,
We_c is the critical Weber number,
La is the Laplace number,
ρ_l is the density of the fuel,
d_d is the incident droplet diameter,
μ is the incident velocity, and
σ is the droplet surface tension.

In the rebound regime, the impinging droplets do not stick to the wall. In the stick and the spread regime, all impinging droplets become part of the wall film. In the splash regime, some of the impinging droplets stick to the wall while others rebound. The split ratio is according to Bai & Gosman:

$$\gamma = \frac{\Delta m_w}{\Delta m_w + \Delta m_{film}} = 0.2 + 0.9a \tag{11}$$

where,
Δm_w is the rebounded mass,
Δm_{film} is the mass transferred to the wall film, and
a is a random number evenly distributed between 0 and 1.

The split ratio can exceed 1 since splashing droplets can entrain droplets from the wall film. In this work, a is set to 0.5 for simplification. The impingement condition for the cylinder wall is set as:

$$S(t) * \cos(\theta) > x_{offset} + (Bore/2) \tag{12}$$

and for the piston as:

$$S(t) * \sin(\theta) > \frac{4 * V_{cylinder}(t)}{\pi * Bore^2} \tag{13}$$

where,
(t) is the spray tip length at the time t,
θ is the spray angle,
x_{offset} is the offset distance from the valve off the cylinder centre, and
$V_{cylinder}$ is the volume of the cylinder at the given time.

The impingement is set to occur for the duration of injection, starting from the time of first impingement. In case the spray tip is slowing down significantly, a delay parameter for the impingement duration is introduced but set to one, since the impingement is occurring very shortly after the injection. Furthermore, a condition is introduced to allow impingement only to the piston or the cylinder exclusively, in case both impingement conditions are fulfilled.

The wall film is calculated the following way:

$$m_{film} = \int_{impingement\ start}^{impingement\ end} \frac{f_{shape} * n_{nozzle} * v(t) * A_{spray}(t) * \rho_{air}(t) * \phi_{eq}(t)}{AFR_{stoich}} dt \quad (14)$$

where,
f_{shape} is a constant set to 0.32 (accounts for the conical shape of the equivalence ratio),
n_{nozzle} is the number of nozzles,
$v(t)$ is the speed of the spray tip,
A_{spray} is the area of the spray front,
$\rho_{air}(t)$ is the density of the air,
$\phi_{eq}(t)$ is the equivalence ratio, and
AFR_{stoich} is the stoichiometric air to fuel ratio.

2.1.4 Evaporation Model

The mass flow of evaporation is calculated as follows:

$$\dot{m_d}(t) = c_1 * (\frac{P}{P_{ref}})^{c_2} * (\frac{n_e}{n_{e,ref}})^{c_3} * \ln(1 + B_M(t)) \quad (15)$$

$$B_M = \frac{Y_{fs}(t) - Y_\infty}{1 - Y_{fs}(t)} \quad (16)$$

$$Y_{fs}(t) = \frac{1}{1 + \frac{AFR_{stoich}}{\phi(t)}} \quad (17)$$

$$Y_\infty = \frac{1}{1 + AFR} \quad (18)$$

where,
c_1, c_2, c_3 are fitting parameters,
P is the power of the engine in [W],
P_{ref} constant set to 1.3063e3 [W],
n_e is the speed of the engine,
$n_{e,ref}$ constant set to 1200 rpm,
B_M is the Spalding mass transfer number,
Y_{fs} is the fuel mass fraction at the droplet surface, and
Y_∞ is the fuel mass fraction in the surrounding charge.

The influence factors for evaporation in this model are the cylinder temperature and the relative speed of the droplets in the wall film to the surrounding air speed. Additionally, the influence of the difference between the local and global fuel mass fraction is included, as it was in Su et al. [7]. The cylinder temperature is assumed to be a function of the engine power. The influence of the relative speed between the droplet and the cylinder air is assumed to be a function of engine speed.

2.1.5 Critical Fuel Mass

The critical fuel mass for soot formation is a combination of the wall film fuel mass and the partially mixed fuel mass both measured at the start of combustion.

$$m_{critical} = m_{wall\ film@SOC} + m_{paritally\ mixed@SOC} \tag{19}$$

$$m_{wall\ film@SOC} = m_{film} - \int_{t(impingement\ start)}^{t(SOC)} \dot{m}_d(t)dt \tag{20}$$

$$m_{wall\ film}(t) \geq 0 \tag{21}$$

The partially mixed fuel mass left in the cylinder is assumed to be a function of turbulence, which is taken as a function of engine speed. For this formula, it is assumed that at low loads, when only a small amount of fuel is injected, all the impinged fuel would evaporate:

$$m_{paritally\ mixed@SOC} = d_1 * n_{engine} + d_2 \tag{22}$$

where, d_1, d_2 are fitting parameters, and n_{engine} is the engine speed.

The parameters are fitted using the insights from measurements and detailed 3D CFD calculations from other tasks of WP1. One example of the comparison data is shown in Figure 2-4. The red marked picture shows the fuel mass film from 3D simulation, the blue marked picture shows the experiments.

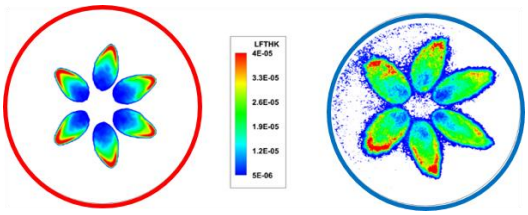

Figure 2-4 Validation data from detailed simulation (red) and experiments (blue)

Figure 2-5 shows the fuel mass over crank angle at the piston or the cylinder liner for a sample operating condition (2000 rpm, start of injection (SOI) at 330° bTDC). The darkest green shows injected fuel mass, the lime green shows the fuel mass, which is impinged on the wall. The remaining green shows the fuel mass, which sticks at the wall. The black line shows fuel mass after evaporation in comparison to the detailed simulation and the experiment.

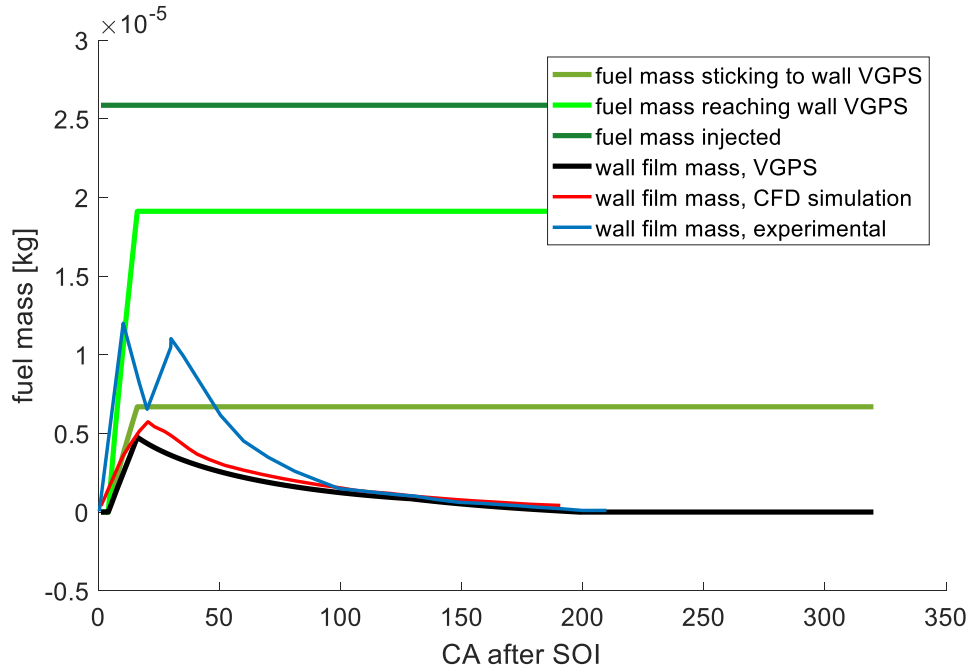

Figure 2-5 Evaporation of the mass film in the vGPS in comparison to measurements and 3D Simulation of the optical engine single cylinder engine

The critical fuel mass is estimated with the wall film fuel mass and the fuel rich portion of the spray at the start of combustion.

2.1.6 Combustion Model

The Vibe (also known as Wiebe) function (equation 23, [8]), has been used to describe the combustion process.

$$\frac{dQ}{d\varphi} \approx k \cdot (-a) \cdot (m_v + 1) \cdot \left(\frac{\varphi}{\Delta\varphi_v}\right)^{m_v} \cdot \exp\left\{a \cdot \left(\frac{\varphi}{\Delta\varphi_v}\right)^{(m_v+1)}\right\} \tag{23}$$

The factor $\Delta\varphi_v$ describes the spread in crank angle direction (duration of combustion), the exponent m_v defines the form of the function ($m_v = 2$ results in a symmetric form, $m_v < 2$ shifts the maximum towards left), and *k* scales the entire form and is proportional to the energy input. The factor a is fixed at $-6.9\frac{\mathrm{J}}{^\circ\mathrm{KW}}$ according to [8]. Here, for sake of simplicity, the heat release was assumed to be symmetric, leading to m_v equal to two. The variable φ_v is depending on the turbulent flame speed, which is estimated, using the mean piston speed, the equivalence ratio as well as compression pressure and temperature. The heat release does not start directly after start of combustion (SOC) since, at the spark timing, the flame front is still moving at the much slower laminar flame speed. The transition from the laminar speed to turbulent speed was thus introduced with the delay factor *L* (fixed at with 8°CA due to very limited sensitivity).

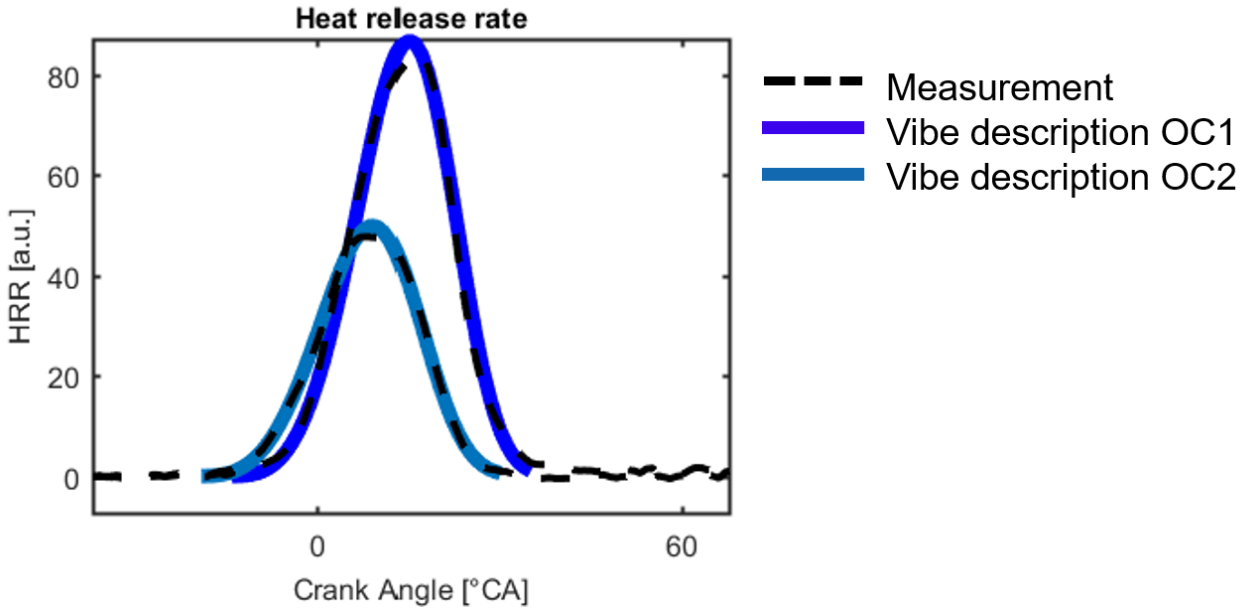

Figure 2-6 Vibe model (blue) in comparison with the apparent heat release rate (black dotted) of two sample operating conditions, estimated with the measured cylinder pressure

2.1.7 Heat Transfer Model

The calculation of the combustion is required for two reasons: first, the heat release rate provides the combustion progress, which is an input for the soot model and, second, the cylinder pressure and temperature can only be estimated knowing the heat release rate in combination with the heat losses through the cylinder wall. The heat losses are included in the heat capacity ratio γ. They are modified as a function of engine speed, load and equivalence ratio.

$$\frac{dp_{i+1}}{d\varphi} = \frac{\gamma - 1}{V}\left(\frac{dQ}{d\varphi} - \gamma \cdot p_i \cdot \frac{dV}{d\varphi}\right) \tag{24}$$

$$p_{i+1} = p_i + \frac{dp_{i+1}}{d\varphi} \tag{25}$$

The cylinder pressure needs to be calculated iteratively, the overall in-cylinder temperature can be estimated with ideal gas law, the unburned temperature though polytropic change of conditions.

2.2 Model calibration

For the calibration procedure of the model, the majority of the parameters are set to the best knowledge from using the Bosch single cylinder (not the optical) engine under 12 operating conditions. Only five parameters have been modified to adapt for a different engine:

- P1: Spray angle factor
- P2: Fuel evaporation factor (c_1 in equation 15)
- P3: Soot formation factor (b_1 in equation 4)
- P4: Spray fuel mass radial distribution factor
- P5: Soot oxidation factor (b_6 in equation 7)

One additional parameter (P6) has been introduce to account for colder walls at cold start or due to direct water injection, which could not have been tested due to lack of data.

P1 to P5 are optimized for the single cylinder Bosch engine, using 25 steady state operating conditions (the initial 12 operating conditions under stoichiometric conditions and additional 13 operating conditions under lean and fuel rich conditions). Furthermore, the model has been calibrated for the engine of the JLR demonstrator vehicle (no data available readily for the engine of the Daimler demonstrator vehicle). This model is calibrated using approximately 80 stoichiometric steady state operating conditions and approximately 50 lean operating conditions.

3 Results

This chapter shows the results of the vGPS calibration on the Bosch single cylinder engine (the calibration for the demonstrator vehicle engine is confidential) and the results of the vGPS integration into the Simulation software Siemens Simcenter Amesim using a sample mean value engine model.

3.1 Single Cylinder Engine

The Figure 3-1 shows a comparison of the results (PN concentrations) from the vGPS and the measurements. The results of the simulation through vGPS are in very good agreement with the measurements (R^2 = 0.97). The majority of the points are captured with a very little error. The first point shows a high difference. The reason might result from intake valve impingement and/or flash boiling. The points 22-25 are a repetition of the points 17-20 after an injector tip clearing procedure. Operating condition 20 is very similar to operating condition 25 but with very different results in PN due to the injector tip. The changed results can only be addressed in the vGPS by changing the parameter P1 (spray angle).

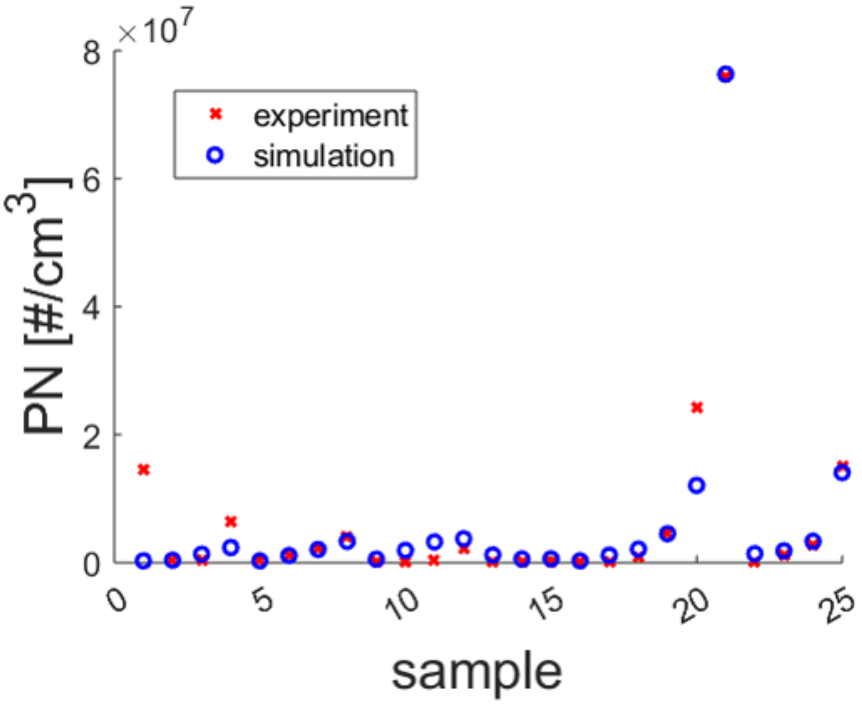

Figure 3-1 Comparison of simulated and measured PN concentration of the single cylinder Bosch engine

3.2 Virtual testing on a sample MVEM

The Figure 3-2 shows PN concentrations over an entire NEDC. The calculations have been performed in the Simcenter Amesim software with the vGPS integrated. A generic mean value engine model has been used.

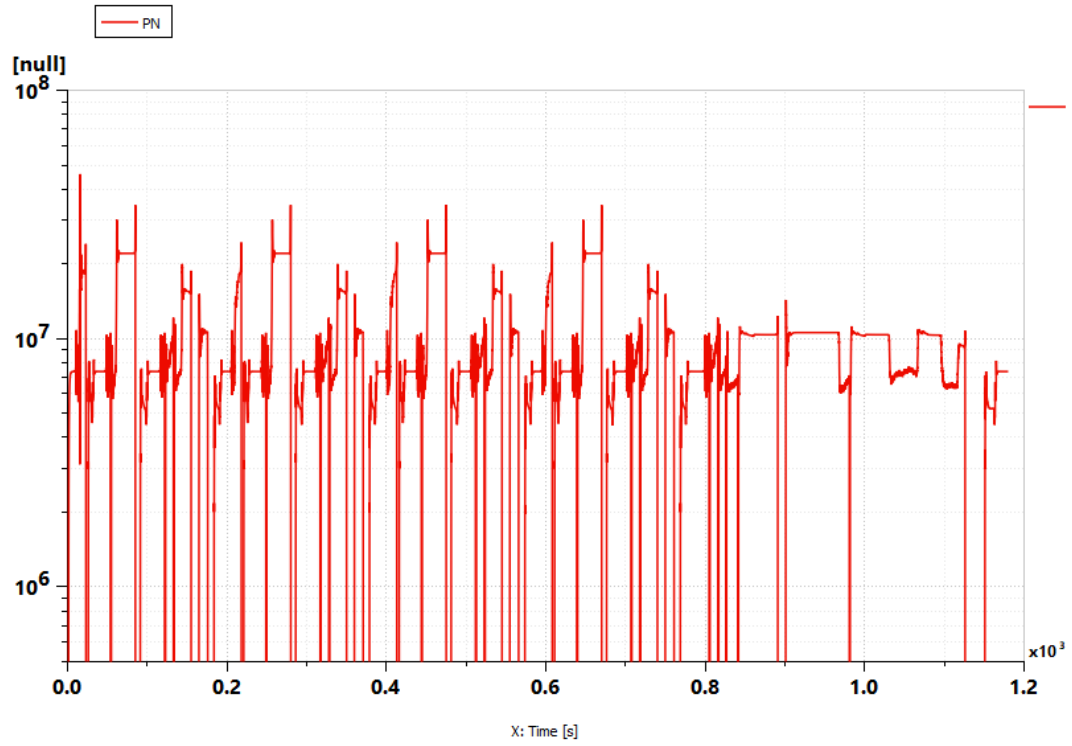

Figure 3-2 PN concentration outputted from AMESIM with the vGPS integrated using a generic mean value engine model

The detailed integration and off-line validation of the vGPS into Amesim is shown in the report of the deliverable D1.8 from Siemens.

4 Summary and Conclusions

A virtual gasoline particle sensor (vGPS) has been developed to enable real-time estimations of the exhaust PM and/or PN from a direct injection spark ignition engine.

The vGPS contains sub-models to describe the dominant phenomena for the soot formation and oxidation processes. The sub-models are used to estimate the fuel mass, which is present under fuel rich conditions, the cylinder pressure and temperature at a time scale suitable as input for a soot model, calculating soot formation and soot oxidation. The phenomena included in the sub-models are air-fuel mixing, wall impingement and evaporation, combustion and heat transfer. Unknowns and engine specific phenomena are addressed with model parameters, which need to be calibrated.

The vGPS has been calibrated for a single cylinder engine as well as a multi cylinder engine under steady state conditions. The engine operation includes stoichiometric, lean and fuel rich conditions. The calculated soot emissions are in good agreement with the measurement results.

The vGPS has been successfully integrated into the simulation software Siemens Simcenter Amesim.

5 Remarks and Deviations

The model code will be sent separately to the Project Officer and the project partners.

There were no specific technical deviations. The report was submitted a day after the date given in the Description of Action as a consequence of the number of deliverables being submitted at that time.

6 Risk Register

Risk No.	What is the risk?	Probability of risk occurrence*1*	Effect of risk*2*	Solutions to overcome the risk
WP1.12	Validation Data is not available	2	2	Validation of procedure and online capability using Siemens Amesim Software

[1] Probability risk will occur: 1 = high, 2 = medium, 3 = Low

[2] Effect when risk occurs: 1 = high, 2 = medium, 3 = Low

7 References

1. Hiroyasu, H. "Diesel Engine Combustion and its Modeling". in *1st International Symposium on Diagnostics and Modeling of Combustion in Internal Combustion Engines*. 1985.
2. Barro, C., Obrecht, P., and Boulouchos, K., "Development and validation of a virtual soot sensor: Part 1: steady-state engine operation." *International Journal of Engine Research*, 2014. **15**(6): p. 719-730, doi: 10.1177/1468087413512309.
3. Barro, C., Obrecht, P., and Boulouchos, K., "Development and validation of a virtual soot sensor: Part 2: Transient engine operation." *International Journal of Engine Research*, 2015. **16**(2): p. 127-136, doi: 10.1177/1468087414533786.
4. Naber, J.D. and Siebers, D.L., "Effects of Gas Density and Vaporization on Penetration and Dispersion of Diesel Sprays". 1996, SAE International, doi: 10.4271/960034.
5. Musculus, M.P.B. and Kattke, K., "Entrainment Waves in Diesel Jets." *SAE International Journal of Engines*, 2009. **2**(1): p. 1170-1193, doi: 10.4271/2009-01-1355.
6. Bai, C. and Gosman, A.D., "Mathematical Modelling of Wall Films Formed by Impinging Sprays". 1996, SAE International, doi: https://doi.org/10.4271/960626.
7. Su, H., Mosbach, S., Kraft, M., Bhave, A., et al., "Two-stage Fuel Direct Injection in a Diesel Fuelled HCCI Engine". 2007, SAE International, doi: https://doi.org/10.4271/2007-01-1880.
8. Vibe, I.I., "Brennverlauf und Kreisprozess von Verbrennungsmotoren". 1970, Berlin: VEB Verlag Technik.

Appendix A – Acknowledgement

The author(s) would like to thank the partners in the project for their valuable comments on previous drafts and for performing the review.

Project partners:

#	Partner	Partner Full Name
1	RIC	RICARDO UK LIMITED
2	DAI	DAIMLER AG
3	JLR	JAGUAR LAND ROVER LIMITED
4	BOSCH	ROBERT BOSCH GMBH
5	FEV	FEV EUROPE GMBH
6	JM	JOHNSON MATTHEY PLC
7	HON	HONEYWELL, SPOL. S.R.O.
8	JRC	JOINT RESEARCH CENTRE – EUROPEAN COMMISSION
9	UNR	UNIRESEARCH BV
10	IDIADA	IDIADA AUTOMOTIVE TECHNOLOGY SA
11	SIEMENS	SIEMENS INDUSTRY SOFTWARE SAS
12	LOGE	LUND COMBUSTION ENGINEERING LOGE AB
13	ETH	EIDGENOESSISCHE TECHNISCHE HOCHSCHULE ZUERICH
14	UDE	UNIVERSITAET DUISBURG-ESSEN
15	RWTH	RWTH AACHEN UNIVERSITY
16	UFI	UFI FILTERS SPA
17	UOB	UNIVERSITY OF BRIGHTON
18	GARR	GARRETT–ADVANCING MOTION

This project has received funding from the European Union's Horizon2020 research and innovation programme under Grant Agreement no. 723954.